

MIT Open Access Articles

*Azimuthal offset#dependent attributes applied
to fracture detection in a carbonate reservoir*

The MIT Faculty has made this article openly available. **Please share**
how this access benefits you. Your story matters.

Citation: Shen, Feng et al. "Azimuthal Offset#dependent Attributes Applied to Fracture Detection in a Carbonate Reservoir." *GEOPHYSICS* 67.2 (2002): 355–364. © 2002 Society of Exploration Geophysicists

As Published: <http://dx.doi.org/10.1190/1.1468596>

Publisher: Society of Exploration Geophysicists

Persistent URL: <http://hdl.handle.net/1721.1/108329>

Version: Final published version: final published article, as it appeared in a journal, conference proceedings, or other formally published context

Terms of Use: Article is made available in accordance with the publisher's policy and may be subject to US copyright law. Please refer to the publisher's site for terms of use.



Case History

Azimuthal offset-dependent attributes applied to fracture detection in a carbonate reservoir

Feng Shen*, Jesus Sierra[†], Daniel R. Burns**, and M. Nafi Toksöz**

ABSTRACT

Offset-dependent attributes—amplitude versus offset (AVO) and frequency versus offset—are extracted from 2-D *P*-wave seismic data using the multiple signal classification technique. These attributes are used to detect fracture orientation in a carbonate reservoir located in the Maporal field in the Barinas basin of southwestern Venezuela. In the fracture normal direction, *P*-wave reflectivity is characterized by a large increase of amplitude with offset (large positive AVO gradient) and a large decrease of frequency with offset (large negative frequency versus offset gradient). In the fracture strike direction, *P*-wave reflectivity shows a scattered variation in AVO but a small variation in frequency with offset. Our results also show that the reservoir heterogeneity can lead to large variations of AVO signatures and that using azimuthal offset-dependent frequency attributes can help lessen the ambiguity when detecting fracture orientation.

INTRODUCTION

With advanced horizontal drilling technology, detecting fracture orientation is very important. Well logs can be used to detect fractures, but they are limited to well locations. Geologic observations can be used to predict fracture orientation but only with certain assumptions. It is known that vertically aligned fractures in a reservoir can induce seismic anisotropy (Lynn et al., 1995). Seismic data have wider spatial coverage than well data; thus, fracture detection using seismic data becomes important for practicality. Shear-wave splitting is very

sensitive to fracture orientation and density. However, the high cost of acquiring multicomponent data makes this method expensive to apply on a regular basis. Using *P*-wave data to detect fractures is very promising and has been of growing interest to the exploration geophysical community.

Studies show that the effect of vertically aligned fractures on *P*-wave propagation is a function of offset and cannot be detected with conventional normal incident seismic data. For this reason, fracture detection based on seismic data analysis has been extended to the prestack domain. Determining fracture orientation from *P*-wave data presently depends on velocity analysis for different common midpoint (CMP) locations and on amplitude versus offset (AVO) analysis for different azimuths. Neidell and Cook (1986) use differential stacking velocity analysis to identify subsurface fracture zones from *P*-wave data. They claim that anomalous velocity zones are related to fractures. Paul (1993) attributes anomalously low stacking velocities to the presence of localized fractures. A similar phenomenon is observed by Lynn et al. (1995) and Corrigan et al. (1996). If a fractured reservoir has a small thickness, the application of *P*-wave stacking velocity is limited because the azimuthal traveltimes depends on both the fracture parameters and the reservoir thickness. In contrast to stacking velocity analysis, azimuthal AVO analysis, relying on the reflection amplitudes, has been used to detect fractures in this case (Perez and Gibson, 1996; Ramos and Davis, 1997; Mallick et al., 1998). Generally, amplitudes are related to reflection coefficients and thus to elastic contrasts across the reflection boundary. Detecting fracture orientation based on azimuthal AVO variations is still ambiguous when a priori information of some variables, such as spatial variations in fluid content, lithology and layer thickness, is not available. Therefore, other seismic attributes, in addition to AVO, are needed to reduce ambiguities and

Manuscript received by the Editor November 12, 1998; revised manuscript received August 27, 2001.

*Formerly Massachusetts Institute of Technology, Earth Resources Laboratory, Department of Earth, Atmospheric, and Planetary Sciences, Cambridge, Massachusetts 02142; presently Peking University, Wave Propagation Laboratory, Department of Geology, Beijing 100871, China. E-mail: sfeng@pku.edu.cn.

†Formerly Massachusetts Institute of Technology, Earth Resources Laboratory, Department of Earth, Atmospheric, and Planetary Sciences, Cambridge, Massachusetts 02142; presently PDVSA—Intevep, Aptdo. 76343, Caracas 1070A, Venezuela. E-mail: sierrajv@pdvsa.com.

**Massachusetts Institute of Technology, Earth Resources Laboratory, Department of Earth, Atmospheric, and Planetary Sciences, 42 Carleton St., Cambridge, Massachusetts 02142. E-mail: burns@mit.edu; toksoz@mit.edu.

© 2002 Society of Exploration Geophysicists. All rights reserved.

constrain solutions in fractured reservoir characterization. Finding additional attributes appears to be feasible in the prestack domain because the seismic signal can be parameterized in terms of amplitude, phase, and frequency versus offset. For example, in the prestack domain, Mazzotti (1991) applies instantaneous amplitude, phase, and frequency versus offset indicators to investigate the possibility of a diagnostic value of seismic data.

Results from 3-D finite-difference modeling shows that fractures tend to decrease the frequency and vary the amplitude of reflected waves at the top of heterogeneously gas-saturated fractured reservoirs. The modeled results also show that the first-order effect of fractures on frequency variations with offset (FVO) and AVO is controlled by the mean fracture density (Shen and Toksöz, 2000). In addition, the study shows that signal frequencies in the crack normal direction decrease faster with offset than those in the crack strike direction. In 3-D seismic applications, Lynn and Beckham (1998) show azimuthal variations in amplitude strength and frequency content associated with a fractured reservoir. Therefore, in addition to azimuthal AVO variation, azimuthal FVO variation could be an indicator of anisotropy.

We introduce a technique, multiple signal classification (MUSIC), for AVO and FVO attribute estimation in the frequency domain using 2-D *P*-wave data and demonstrate the application of these attributes to detecting fracture orientation in a carbonate reservoir in Maporal field, southwestern Venezuela. By combining inverted velocities with calculated reflection coefficients, we investigate effects of reservoir heterogeneity on AVO signatures. Our purpose is to show that, in detecting fracture orientation, including FVO is more beneficial than using AVO alone.

SEISMIC DATA

The Maporal field is located in the Barinas basin of southwestern Venezuela, characterized by a structure dome extending northeast–southwest. The fractured reservoir occurs in member O of the upper Cretaceous Escandalosa Formation and consists of dolomitic carbonate and carbonate. Member O overlies members P and R and is overlain by the La Morita and Gobernador Formations, all mainly composed of sandstone and shale. Based on area well logs, the thickness of member O is about 30 m. Images from formation micro scanner (FMS) logs and wellbore ellipticity analyses identify fractures in the carbonate reservoir.

Two-dimensional, three-component seismic data were acquired in this field. Three 10-km seismic lines with three azimuths intersect over the structural high of the fractured reservoir (Figure 1, including well locations and major faults). The structural high is cut by a normal fault trending northwest–southeast. The other two major normal faults trending northeast–southwest are distributed on northwestern and southeastern sides of the high. Azimuths of lines 1 and 3 are almost parallel to northeast- and northwest-trending normal faults, respectively; line 2 almost bisects lines 1 and 3 and forms an angle of approximate 40° with line 1. A 1-kg explosive charge at 10 m depth was used for the source. The shotpoint spacing was 51 m, and the source offset was 17 m. The nearest offset was 17 m and the farthest offset was 3650 m, equivalent to an incidence angle of 32° for the target zone (Perez, 1997). The

maximum fold was 33 traces. The detailed survey parameters can be found in Table 2 of Ata and Michelena (1995).

The *P*-*S* converted wave data collected in this area exhibit significant amplitude differences between the fast and slow shear-wave components, which are interpreted to be fracture effects (Ata and Michelena, 1995). Based on *P*-*S* converted seismic data and correlation between the seismic and well logs, Ata and Michelena (1995) show that fracture orientation tends to run subparallel to the fault system, and fractures are parallel or subparallel to line 3. The fracture orientation yielded from *P*-*S* data also aligns along the maximum horizontal regional stress, oriented northwest–southeast, consistent with the fracture orientation measured in the wells in the carbonate reservoir. Local variations in fracture orientation derived from 3-D *P*-wave azimuthal AVO also show good correlation with the orientation of maximum horizontal stress (Perez et al., 1999). In this study, 2-D *P*-wave seismic data with three azimuths are used for fracture detection in the carbonate reservoir.

Like acquisition operations, processing operations play an important role in seismic data quality control. Our processing sequence aims to remove distorting effects partially caused by ground coupling of sources and receivers, source–receiver patterns, and near-surface conditions and to increase the S/N ratio. We avoid adaptive processes such as signal–trace deconvolution, spectral whitening, and amplitude scaling. The processing sequence applied to three seismic lines includes spherical divergence correction, *f*-*k* filter, refraction statics, CMP sorting, NMO, and residual statics. After a two-pass velocity analysis, trace editing and bandpass filtering are performed.

Figure 2 shows three stacked seismic sections tied with each other at their intersecting point (CDP 224). The good tie at major reflectors indicates that very little bias is introduced by processing algorithms, so the approximate behavior of reflection amplitudes can be used to estimate offset-dependent attributes. To locate the target zone in the seismic profile, synthetic seismograms are generated from logs that intersect or are close to the seismic lines. On average, the spectral analysis shows that *P*-wave seismic data have a dominant frequency at 25 Hz in the fractured reservoir zone. The wavelet is extracted from well logs and stacked seismic data. Figure 3 shows an example of synthetic seismograms generated with sonic and

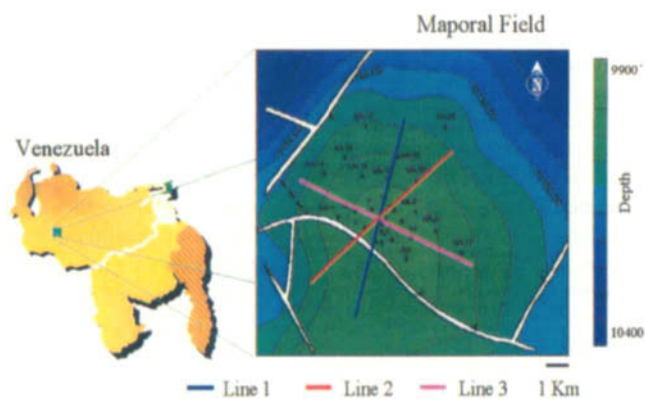


FIG. 1. Structure map of the top of the Escandalosa Formation in the Maporal field, Barinas basin, southwestern Venezuela. Locations of wells and geometry of three seismic survey lines are shown on the map.

density logs at well MA-13 and tied with the stacked seismic section of line 1. The fractured carbonate reservoir is at 3180 m around 2340 ms in the profile and is characterized by strong reflectivity.

ANALYSIS OF OFFSET-DEPENDENT ATTRIBUTES

Attribute estimator

The MUSIC frequency estimator is used to extract seismic attributes in the frequency domain. The introduction of the MUSIC algorithm (Schmidt, 1979) is an attempt to fully exploit the underlying data model. MUSIC has received much attention and can provide asymptotically unbiased estimations of signals. This technique has better resolution and better frequency estimation characteristics than spectral techniques such as autoregressive or Prony methods.

MUSIC is based on an eigenanalysis of a correlation data matrix. It separates information in the correlation matrix into two vector subspaces: one a signal space and the other a noise space. Functions of the vector in either the signal or the noise space can be used to create frequency estimators. The estimated peak value represents the signal strength, and the number of spectral peaks represents the number of signals. Signal locations in the frequency range indicate signal frequencies.

The frequency estimator function is given as

$$F(f) = \frac{1}{\sum_{K=M+1}^P \alpha_K |e^H(f)V_K|^2}, \quad (1)$$

where α is the weighting function, M is the number of signals, P is total eigenvectors, V is an eigenvector, and e is a complex sinusoid vector. The superscript H denotes the Hermitian transpose operation. When $e(f_i) = s_i$, one of sinusoidal signal vectors, the estimation causes function $F(f)$ to have very sharp peaks at signal frequency f_i . The frequency estimator is a pseudospectrum estimator because the correlation sequence cannot be recovered by Fourier transforming the frequency estimator. Setting $\alpha_K = 1$ for all K leads to the multiple signal classification algorithm (Schmidt, 1986); setting $\alpha_K = 1/\lambda_K$ for all K yields the eigenvector algorithm frequency estimator (Johnson and DeGraaf, 1982) where λ_K is the eigenvector associated with V_K . The frequency estimator also is detailed by Shen and Toksöz (2000).

Modeling studies for the carbonate fractured reservoir

To understand how fractures affect AVO responses in our working area, P -wave azimuthal AVO variations are calculated using an approximation reflection coefficient equation (Ruger, 1998). A horizontal two-layer model is built using elastic parameters derived from log data acquired at well MA-17, where P - and S -wave velocities and rock density were measured. Log data in other wells are also considered in building the model. In the Maporal field, the fluid material filling the fracture system is oil and water. The API oil gravity number of the crude is 28 (Perez, 1997). Oil density and modulus are calculated based on Batzle and Wang (1992) with the in-situ temperature and pressure. The effective medium model (Schoenberg and Sayers, 1995) and Hudson's crack models (Hudson, 1981; Hudson et al., 1996) are used to invert the stiffness tensor of a fractured medium, which is studied in detail by Liu et al. (1996). The relationship between stiffness coefficients and fracture parameters is linked with these models. The anisotropy parameters of the equivalent VTI model for HTI media are introduced by Tsankin (1996) and can be represented through stiffness coefficients. The elastic parameters of rocks, fracture parameters, and anisotropy parameters used in modeling are summarized in Table 1.

Our previous studies show that azimuthal AVO variations in fractured reservoirs are influenced by fracture parameters, including fracture density, fluid content, and fracture aspect ratio (Shen, 1999). To investigate how the fluid content and fracture density affect the azimuthal AVO variations in this area, we calculate azimuthal AVO responses. Figure 4 shows the P -wave AVO responses at the top of oil- (28° API) and water-saturated fractured reservoirs. Increasing crack density increases the AVO gradient. Modeled results also show that, with equal fracture density, the oil-saturated fractured carbonate reservoir has a smaller AVO gradient than the water-saturated one. Our results indicate that when fractures are saturated with oil or water, the effect of fractures leads to a large increase in AVO gradient and is a major contributor to azimuthal AVO variations.

As mentioned above, the average thickness of the fractured reservoir in member O is 30 m. Using an average interval velocity of 4400 m/s obtained from sonic logs in the reservoir

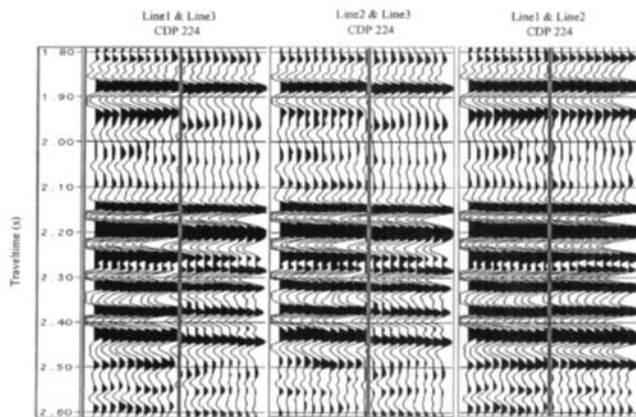


FIG. 2. Tying P -wave sections at their intersection point, CDP 224.

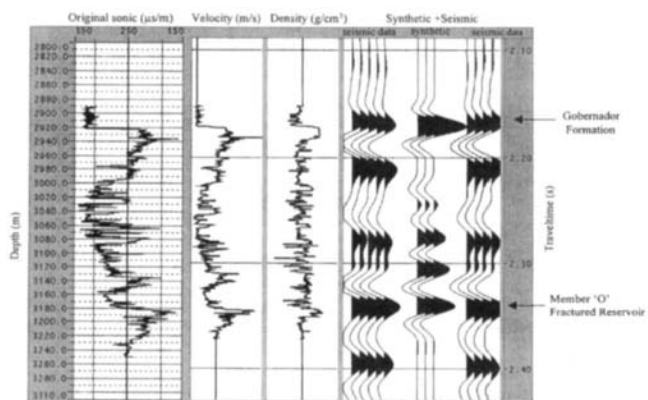


FIG. 3. Synthetic seismograms generated from sonic and density logs at well MA-13 tied with the stacked seismic profile of line 1.

zone and a dominant frequency at 25 Hz, the corresponding tuning thickness is 44 m (with thickness = $H/4$, where H is the wavelength of the seismic pulse at the peak frequency). Since the reservoir in member O is within tuning thickness, elastic properties of formations beneath and above member O could also contribute to the seismic responses of the reservoir. Ramos and Davis (1997) show that when the maximum thickness of a reservoir is smaller than half a wavelength, the variation of reservoir thickness can lead to oscillation in the AVO gradient. Therefore, tuning may add bias in AVO and FVO gradients.

To investigate characteristics of azimuthal variations of AVO and FVO when a fractured reservoir is within tuning thickness, we use elastic coefficients listed in Table 1 and decrease the thickness of the fractured reservoir to $H/4$. For simplicity, the oil-saturated fractured reservoir is assumed to have the same shale/sandstone above and below it. The 3-D time-domain, staggered-grid, finite-difference method is used to obtain seismograms. This method has fourth-order accuracy in space and

Table 1. Elastic parameters, fracture parameters, and anisotropy parameters

Rocks	Shale	Carbonate
V_p (m/s)	3410	4400
V_s (m/s)	2010	2224
ρ (g/cm ³)	2.48	2.6
Fracture density		0.10
Fracture aspect ratio		0.01
Fluid content		oil (API28)
C_{11} (GPa)	28.6051	44.4152
C_{12} (GPa)	8.7278	21.7204
C_{13} (GPa)	8.7278	21.7204
C_{22} (GPa)	28.6051	48.9200
C_{23} (GPa)	8.7278	23.1999
C_{33} (GPa)	28.6051	48.9200
C_{44} (GPa)	9.9386	12.8601
C_{55} (GPa)	9.9386	10.5039
C_{66} (GPa)	9.9386	10.5039
$\epsilon^{(v)}$ (API28)		-0.0460
$\delta^{(v)}$ (API28)		-0.1164
γ (API28)		0.0916
$\epsilon^{(v)}$ (water)		-0.0296
$\delta^{(v)}$ (water)		-0.1062
γ (water)		0.0916
V_p/V_s	1.6965	1.9784

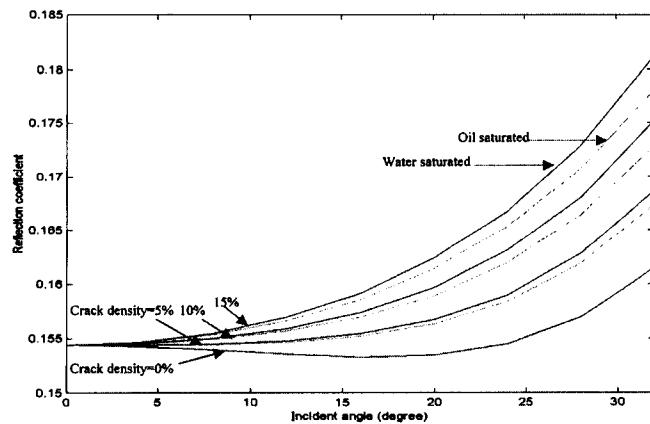


FIG. 4. Calculated AVO responses in oil- (28° API) and water-saturated fractured reservoirs with 0%, 5%, 10%, and 15% fracture density. Parameters are listed in Table 1.

second-order accuracy in time (Cheng et al., 1995). An explosive source (Kelly wavelet) is used; the dominant frequency of the source wavelet is 30 Hz. Seismograms show that azimuthal AVO variations can be observed, and amplitudes in the crack normal direction is larger than those in the fracture strike direction (Figures 5a,b). The frequency decay in the crack normal direction is larger than that in the crack strike direction (Figures 5c,d). In our working area, well-log data show small variations in the reservoir thickness. Therefore, the tuning effect should produce similar changes in the AVO and FVO on three seismic lines, so azimuthal variations of AVO and FVO are valid in detecting fracture orientation.

Seismic data analysis of AVO and FVO and interpretation of fracture orientation

Considering that the fractured reservoir is located around the intersection area of three seismic lines and that the azimuthal comparison of offset-dependent attributes can be made conveniently, a subset of seismic data with a full range of offset is adopted in this study. Three seismic lines intersect each other at CDP 224. Sixty CDPs (221–280) on each line are used in our attribute estimation.

Figure 6 shows processed gathers from CDP 222–226 of three seismic lines. Amplitudes on CDP gathers in the reservoir target zone characteristically increase with offset. Seismic traces in the near and middle offset largely differ from those in the far offset in amplitudes, frequency, and phase. An extra reflected event occurs at the near and middle offset below the reservoir reflectivity but disappears in the far offset. Based on waveform characteristics, we divide seismic traces in CDP gathers of three seismic lines into two groups: near–middle offset and far offset. On average, the offset range is from 17 to 2000 m for the near–middle offset traces, approximately corresponding to the end of

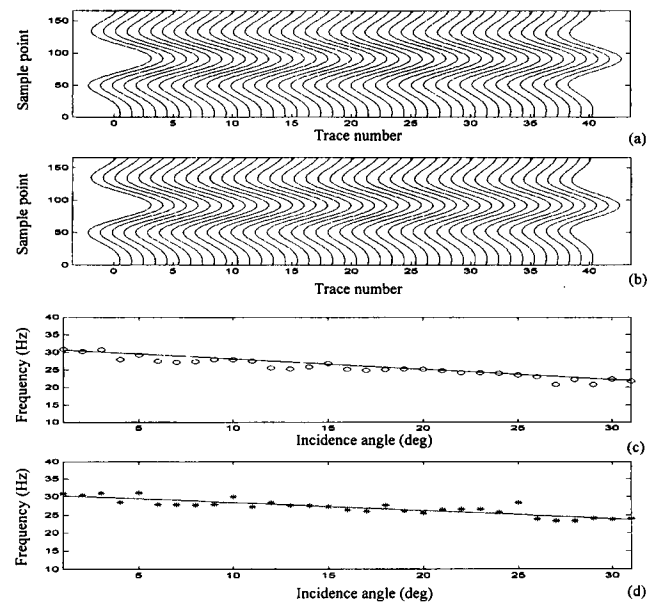


FIG. 5. Seismograms generated from 3-D finite-difference modeling and estimated FVO. (a) Seismograms in (a) the fracture normal direction and (b) the fracture strike direction (sample rate $\Delta t = 0.35$ ms). Estimated FVO in (c) the fracture normal direction and (d) the fracture strike direction.

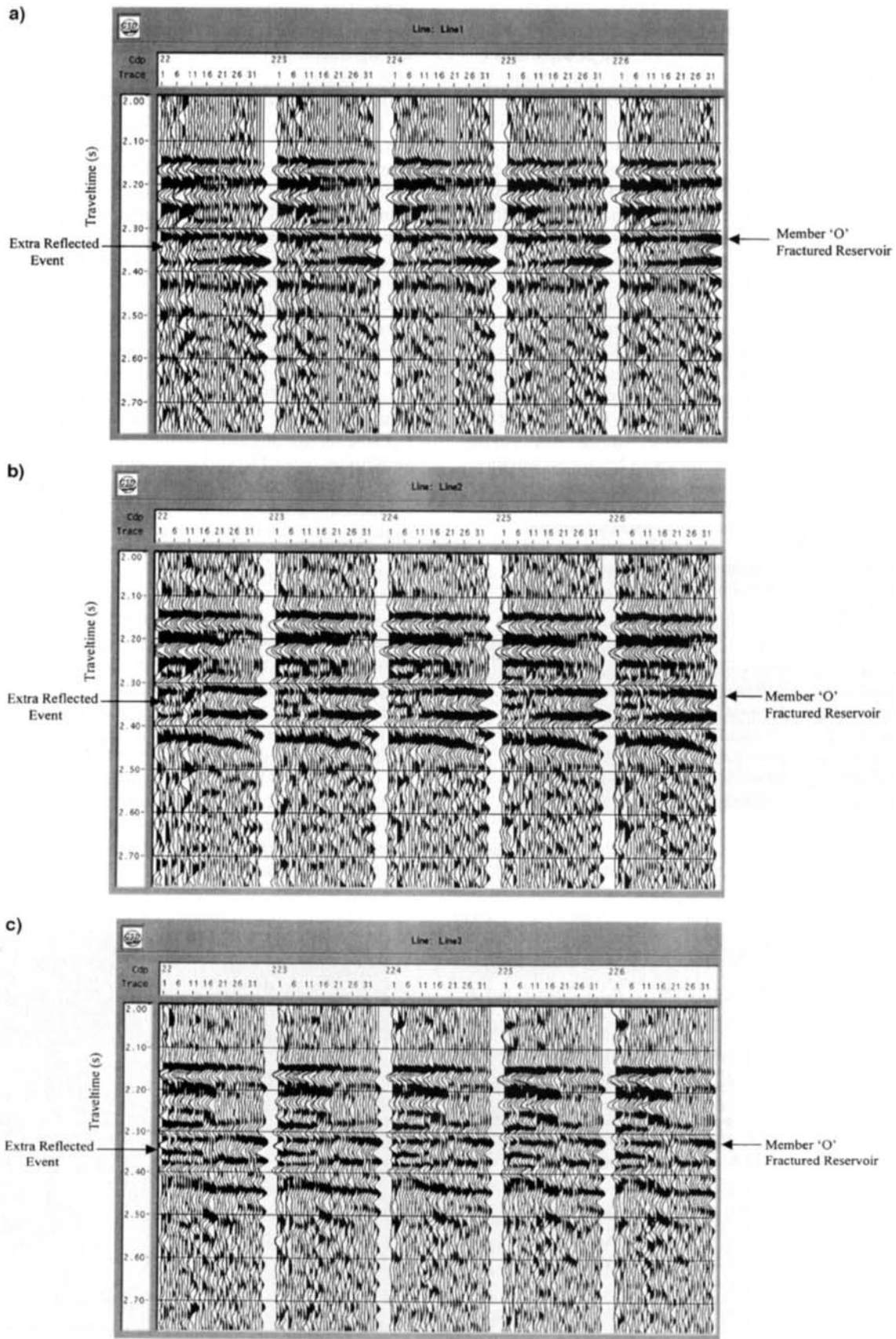


FIG. 6. Prestack CDP gathers; CDP 222–226 on (a) line 1, (b) line 2, and (c) line 3.

the extra reflectivity, and from 2001 to 3650 m for the far-offset ones. Differences in seismic waveforms between near-middle and far-offset traces can also be shown with stacked seismic data. The partial stacked data, stacked with near-middle offset traces, have high frequency in the reservoir zone. The extra reflected event can be observed below the fractured reservoir reflectivity. However, the overall stacked data, stacked with all traces in a CDP gather, are characterized by strong reflectivity and good continuity. The extra reflected event is invisible on three seismic lines (Figure 7). These analyses show there are large variations in the amplitude and frequency from the near-middle to far-offset traces.

To avoid the large variances occurring in the estimation of AVO and FVO gradients when the linear model is used, only far-offset traces are used instead of all traces in a CDP gather. To do so, the offset-dependent AVO and FVO gradients are obtained from fitting with the linear model. As indicated in our fractured reservoir studies, effects of fractures on amplitudes and frequencies of reflected waves in fracture off-strike directions increase with increasing offset. Reflected data in the far offset contain more information about fractures than those

in the near-middle offset (Shen, 1999). Therefore, estimated attributes by using far-offset seismic data are still valid in detecting fractures if these data can cover approximately equal offset ranges.

In our estimation, we use a constant time window of 40 ms for 21 samples, centered around the fractured reservoir. The windowed seismic data actually correspond to the response of an averaged medium composed of carbonates in the reservoir zone and noncarbonate materials (typically shale and sandstone) above and beneath member O. However, the contribution of the interface containing the top of the fractured reservoir to the P -wave reflectivity is greater than any other interfaces above and beneath the reservoir zone. MUSIC is used to extract amplitude and frequency attributes from windowed seismic waveforms in CDP gathers.

Figure 8 shows three CDP gathers and their locations on the seismic lines. Figure 9 shows their normalized AVO (signal energy) and FVO. A linear regression, based on least absolute deviations, is used to obtain AVO and FVO gradients. Because we are interested in the gradient of AVO, the P -wave amplitudes in a CDP gather are normalized by the amplitude of the smallest offset. This normalization does not affect the comparative analysis in azimuthal AVO variations. The AVO signatures are relative values and do not correspond to direct measurements of rock properties.

The P -wave azimuthal AVO and FVO analyses are made on all 180 CDPs of three seismic lines. Distributions of all CDPs in attribute space, consisting of AVO and FVO gradients, are shown in Figure 10a. Statistic characteristics of CDPs on each seismic line are shown in Figures 10b–d, pair by pair. CDPs on line 1 are characterized by a large increase in amplitude with offset and a large frequency decrease with offset. Those on line 2 show a small increase in amplitude with offset and a moderate frequency decrease with offset. And those on line 3 are characterized by a scattered variation in AVO but a small variation in FVO. If azimuthal variations of offset-dependent amplitude and frequency attributes on three seismic lines are caused by fractures, these attributes could be used to detect fracture orientation.

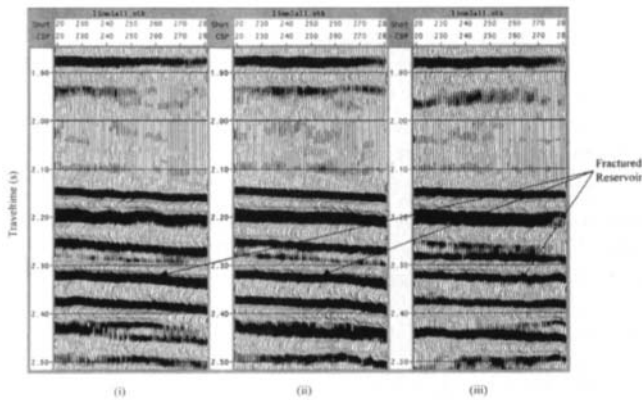


FIG. 7. Overall stacked seismic profile, stacked with full-range offset data on (i) line 1, (ii) line 2, and (iii) line 3.

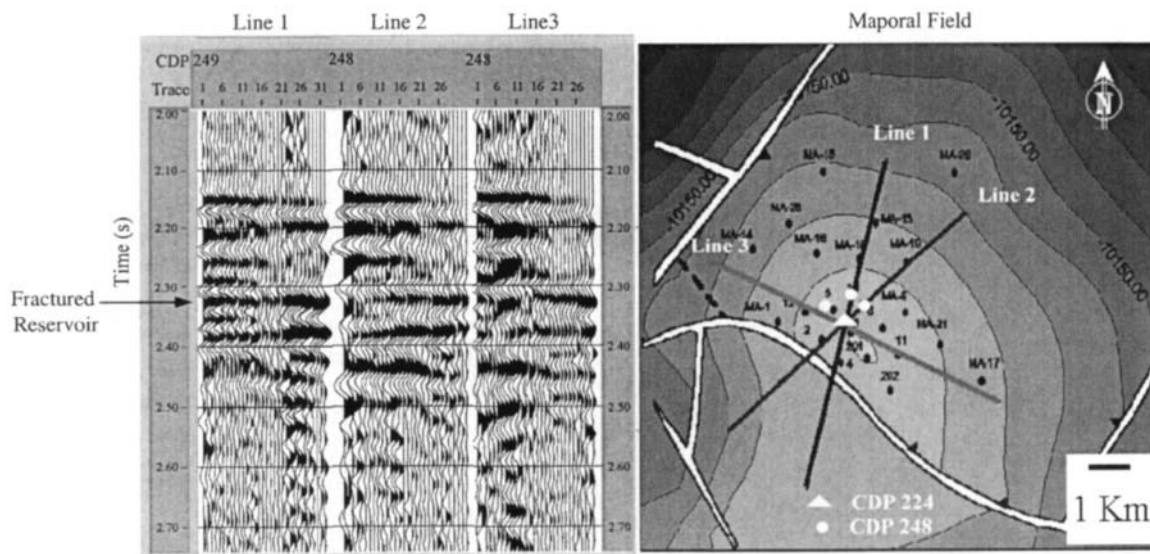


FIG. 8. CDP gathers on line 1 (CDP 249), line 2 (CDP 248), and line 3 (CDP 248) and their locations on the structure map.

With the help of our modeled AVO and FVO responses to fracture effects in the Maporal field, we try to relate clusters of AVO and FVO gradients to the fracture orientation. Based on characteristics of AVO and FVO gradients, line 1 is the most perpendicular to the fracture orientation and line 3 is the most parallel to the fracture orientation. Since the characteristics of AVO and FVO gradients on line 2 are close to those of line 1, line 2 should be the line near perpendicular to the fracture orientation. This interpretation yields a similar regional trend as that obtained previously from P - S converted wave data (Ata and Michelena, 1995) and is consistent with the fracture orientation measured in the wells around the carbonate reservoir and the orientation of maximum horizontal stress.

Effects of reservoir heterogeneity on AVO signatures

The scattered AVO gradients on line 3 lead to an important conclusion concerning the reservoir heterogeneity caused by

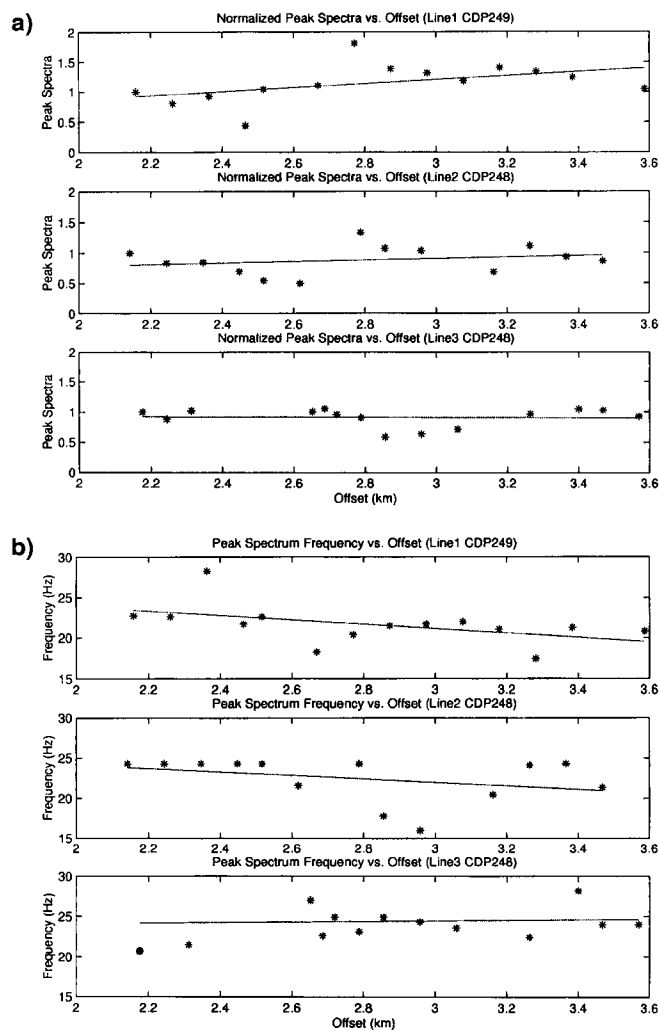


FIG. 9. (a) Estimated normalized AVO (signal energy) from the top to the bottom, CDP 249 (line 1), CDP 248 (line 2), and CDP 248 (line 3). (b) Estimated normalized signal frequencies versus offset from the top to the bottom, CDP 249 (line 1), CDP 248 (line 2), and CDP 248 (line 3).

spatial variations in lithology. As we know, seismic data near normal incidence provide information about the changes in acoustic impedance between adjacent layers. Poisson's ratio is the elastic property most directly related to angular dependence of reflection coefficients. To investigate whether the scattered AVO gradients occurring on line 3 are caused by lithology-related heterogeneity in the reservoir zone, we invert interval velocities from partial stacked data of near-middle offset.

Velocity inversion is performed with a commercially available package (RICH). The wavelet is extracted based on the amplitude spectrum of a selected time window from stacked seismic data and on a scan of the phases to pick one that best matches synthetic and true seismic traces. Since vertical fractures have very little effect on near-offset seismic data, velocities inverted from partial stacked data are mostly related to reservoir acoustic properties. In line 1, inverted velocities smoothly decrease from low to high CDP numbers in the fractured reservoir zone (Figure 11a). Line 2 shows small lateral variations in velocities, and high velocities are distributed between CDP 236 and 260 (Figure 11b). In contrast to lines 1 and 2, velocities in line 3 show significant lateral variations and indicate strong heterogeneity occurring in the reservoir zone (Figure 11c). High velocities distribute along ranges in both high and low CDP numbers, from 200 to 228 and from 264 to 300. At the intersecting point (CDP 224), velocities inverted from partial stacked data of three seismic lines can be tied well. The good tie confirms that lateral velocity variations in line 3 result from the reservoir heterogeneity. Since line 3 is parallel to the fracture orientation, the scattered AVO gradients in far-offset amplitudes could be caused by the heterogeneity of reservoir acoustic properties.

To obtain insight into how the reservoir heterogeneity affects P -wave AVO variations (equivalent AVO variations in the fracture strike direction), we calculate the P -wave reflection coefficients at incidence angles of 0° and 32° and then normalize them with the reflection coefficient at the 0° incidence angle. The difference of normalized reflection coefficients between incidence angles of 0° and 32° is approximately proportional to the AVO gradient. Based on our inverted velocities, we use 1-D stochastic modeling (Goff and Jordan, 1988) to build the velocity variation profile and let the velocity vary ± 350 m/s around a reservoir mean velocity of 4400 m/s. Two cases are considered in our calculations when the reservoir is assumed to be oil saturated and with 10% fracture density. In case 1, the Poisson's ratio is constant with variable P -wave velocity (V_p). In case 2, the S -wave velocity (V_s) is constant with a variable Poisson's ratio. In case 1, AVO gradients decrease with the increase of V_p from 0.1642 to -0.0186 (Figure 12a). In case 2, with the increase of V_p , varying Poisson's ratio leads to a large variation in AVO gradients from -0.1189 to 0.1343 (Figure 12b). Our results show that two cases give rise to large variations in AVO signatures at an incidence angle of 32° . Therefore, the reservoir lateral heterogeneity could be a major contribution to the scattered variation in AVO gradients on line 3.

Additionally, if the reservoir is assumed to be water saturated with 10% in fracture density, the AVO gradients in the fracture normal direction for the two cases are also calculated (Figure 12). Our results show that water-saturated fractured reservoirs have larger azimuthal AVO variations than

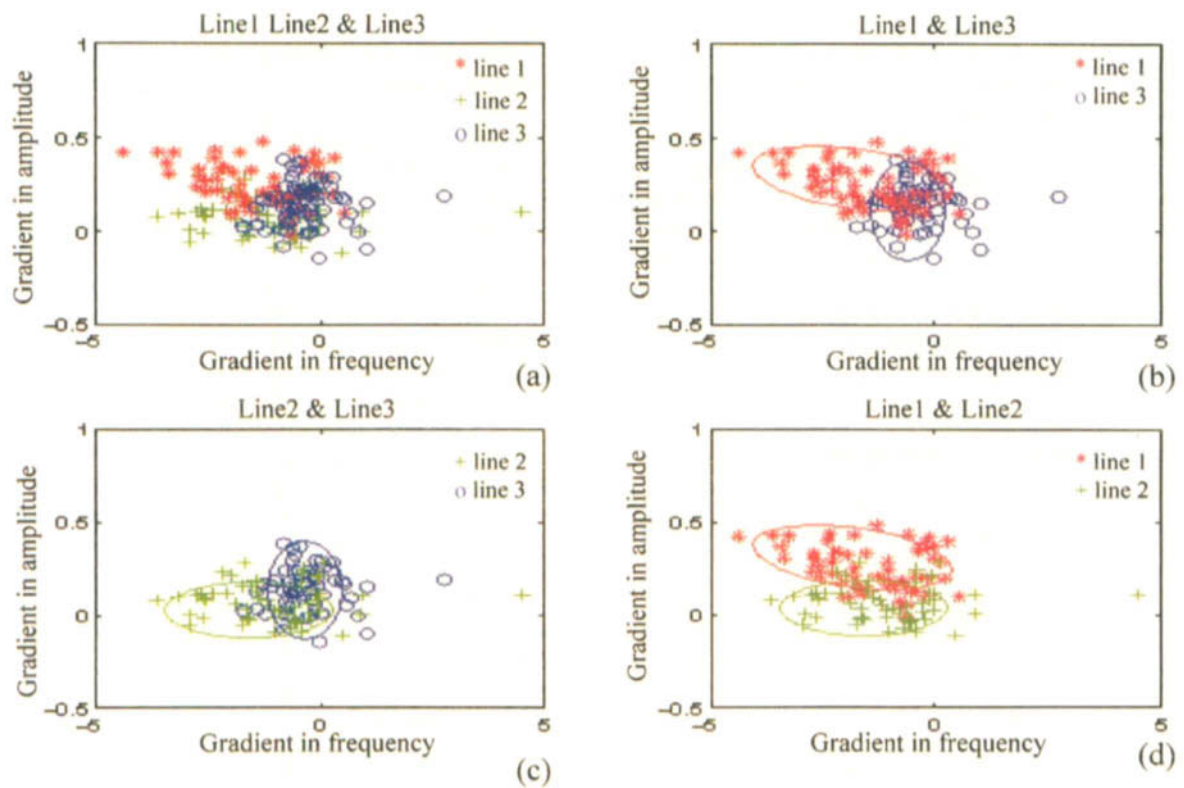


FIG. 10. (a) Distributions of estimated AVO and FVO gradients in the attribute space. Characteristics of AVO and FVO gradients of (b) lines 1 and 3, (c) lines 2 and 3, and (d) lines 1 and 2 in the attribute space.

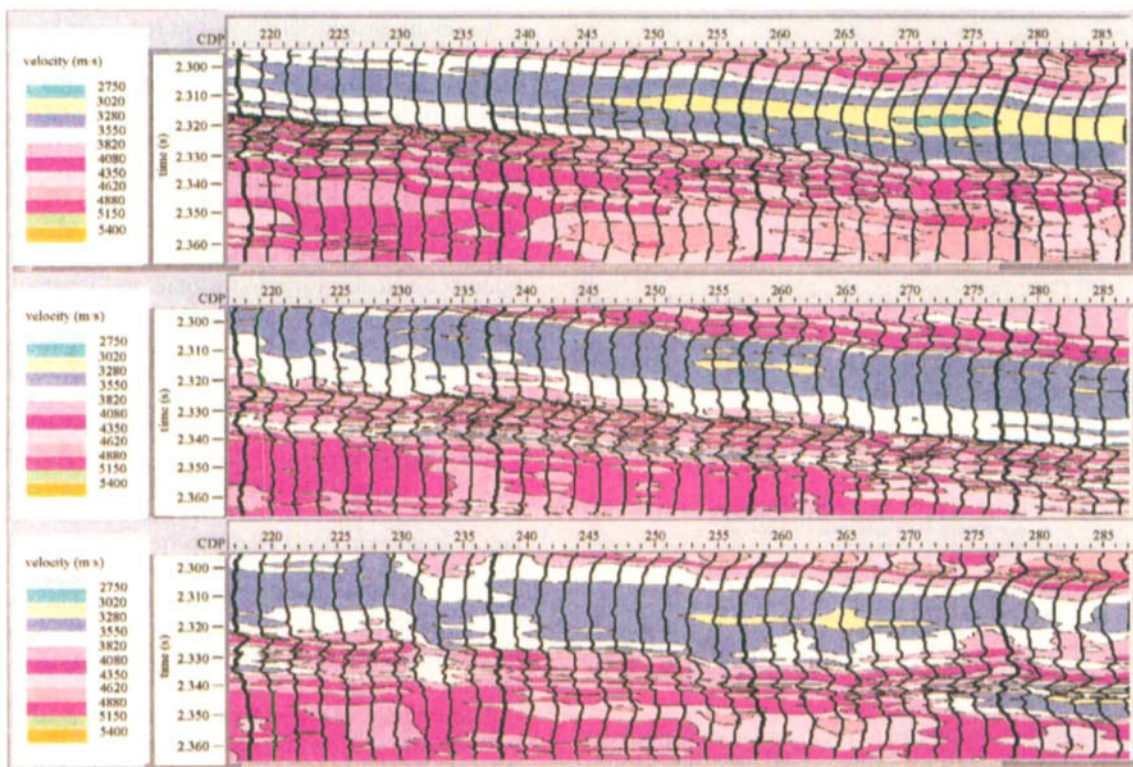


FIG. 11. (a) Inverted P -wave velocities from partial stacked data on (a) line 1, (b) line 2, and (c) line 3. The arrow indicates the traveltime location of the fractured reservoir.

oil-saturated ones. If the difference in AVO gradients between the fracture normal and strike directions can be an indicator of azimuthal AVO variations, varying P -wave velocities can also lead to variations in azimuthal AVO responses when fractures are oil or water saturated. The variable Poisson's ratio in the reservoir zone has a larger effect on azimuthal AVO variations than the constant one. These results also suggest that the azimuthal AVO signatures are not necessarily correlated with fracture parameters and that reservoir heterogeneity should be considered in fractured reservoir characterization.

DISCUSSION AND CONCLUSION

We have demonstrated that AVO and FVO attributes estimated from waveforms of P -wave data can be used to help detect fracture orientation in reservoirs within tuning thicknesses. These attributes are selected based on their capability of providing physical relationships between the fracture effects and the seismic responses. In addition, estimation based on seismic waveforms is less sensitive to errors caused by residual velocity and inaccurate static correction. Statistical analysis in the attribute space is very helpful for identifying major characteristics of estimated attributes, particularly when the number of wells is limited and it is not possible to carry out quantitative calibrations.

In the Maporal field fractured reservoir, fractures are a major contribution to azimuthal AVO variations, and increasing fracture density gives rise to a large increase in AVO gradients. For an oil-saturated fractured reservoir with the tuning thickness, the presence of fractures leads to a large frequency decrease with offset. Our data analysis results show that the CDPs on line 1 are characterized by a large increase in amplitudes with offset and a large frequency decrease with offset. Line 2 is characterized by a moderate frequency decrease with offset and a small amplitude increase with offset. CDPs on

line 3 are characterized by a scattered variation in AVO and a small variation in FVO. Relating the statistic signatures of AVO and FVO to the fracture orientation, we find line 1 is the most perpendicular to the fractures, while line 3 is the most parallel to the fractures. Since the characteristics of seismic attributes on line 2 are comparable with those on line 1, line 2 is nearly perpendicular to the fractures. Therefore, knowledge of the amplitudes and frequency variations with offset provides a better understanding of the effects of fractures on P -wave reflected data and yields further information about a reservoir's properties.

Both fracture parameters (fracture density, saturated fluid content, and fracture aspect ratio) and nonfracture parameters (V_p , V_s , and Poisson's ratio of background rocks) can result in variations in AVO signatures. Our results show that increasing fracture density and changing the fluid content from oil to water can lead to a large azimuthal AVO response. Parra et al. (2000) show that as long as there is fluid flow in the rock matrix toward the cracks, the fluid motion will attenuate the acoustic/seismic waves. Different fluid content may have different contributions to the attenuation. Therefore, inclusion of the frequency attribute is more beneficial than using amplitude alone in fracture reservoir characterization.

For nonfracture parameters, modeled results show that variations in Poisson's ratio and P -wave velocity in the reservoir zone can give rise to large variations in AVO gradients. Therefore, the lithology-related reservoir heterogeneity has an important effect on AVO signatures. Although azimuthal AVO variations have been used successfully in fracture detection, our studies indicate that it is worthwhile to combine AVO analysis with FVO analysis and that information about frequency varying with offset can help lessen the ambiguity in fracture detection. Modeling studies are very important; they can help us understand the physical meaning of estimated attributes and better interpret fracture orientation.

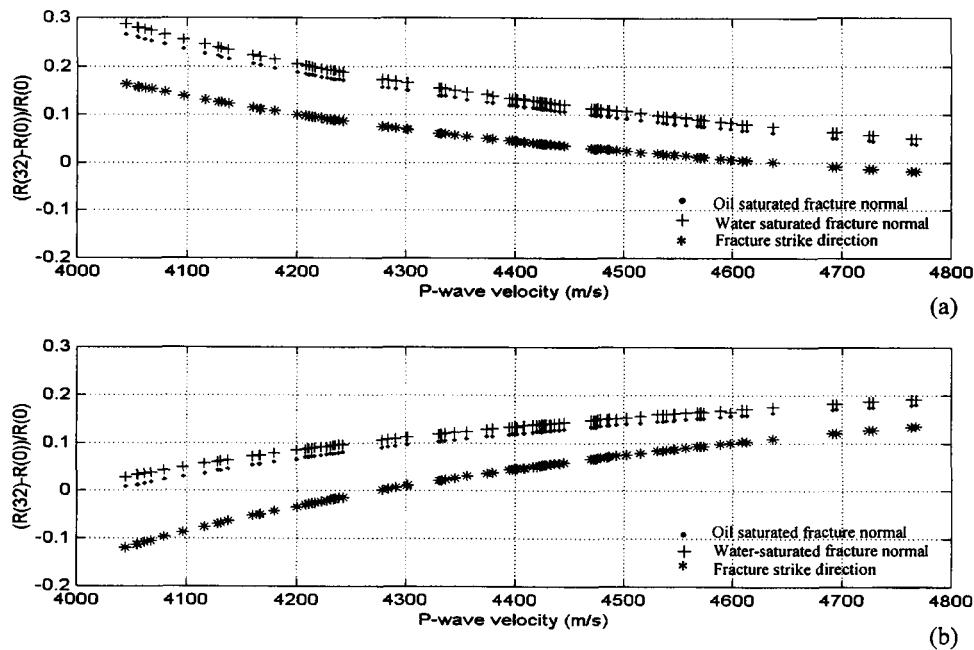


FIG. 12. (a) AVO gradients $[(R(32^\circ) - R(0^\circ))/R(0^\circ)]$ as a function of P -wave velocities in the oil- and water-saturated fracture normal and strike directions in (a) case 1 (constant Poisson's ratio) and (b) case 2 (variable Poisson's ratio).

To check the estimated results qualitatively, rms amplitudes are calculated and AVO gradients are obtained by straight-line fitting in windowed seismic waveforms in the time domain. The lateral variations in AVO gradients from these two estimation methods are approximately consistent on the three seismic lines, which confirms the reliability of the frequency estimator.

Errors from estimation and physical interferences in seismic data can contribute to distortion of the AVO and FVO gradients and intercepts. To check the validity of the straight-line fit and the oscillation in the amplitudes and frequency data, the mean absolute deviation from the fit lines is one criterion for measuring reliability. Studies from Ramos and Davis (1997) show that undulations in the normalized rms amplitude data are caused by converted waves and coherent noise. Additionally, the CDPs with very limited offset ranges have a small degree of reliability. These errors should be considered when making interpretations using estimated attributes.

ACKNOWLEDGMENTS

We acknowledge valuable help from Maria Perez at Intevep S.A. Venezuela in our seismic data processing. We thank Franklin Ruiz at M.I.T. for helpful discussions. The comments and suggestions of the *Geophysics* reviews (Heloise Lynn and anonymous reviewers) are appreciated. Special thanks to the associate editors for their constructive reviews of the paper. We specifically thank Intervep S.A. for providing us with seismic data. We very much appreciate GeoSoft Development Inc. of the China National Petroleum Corp. (CNPC) for providing us with a research facility and support in our velocity inversion. This research was supported by the Borehole Acoustics and Logging/Reservoir Delineation Consortium at M.I.T. It was also supported by grants from the National Science Foundation of China (D0409, 49974032) and was a key project for basic research on oil basins (G19990433(11)).

REFERENCES

- Ata, E., and Michelena, R. J., 1995, Mapping distribution of fractures in a reservoir with *P-S* converted waves: *The Leading Edge*, **12**, 664–676.
- Batzle, M., and Wang, Z., 1992, Seismic properties of pore fluids: *Geophysics*, **57**, 1396–1408.
- Cheng, N., Cheng, C. H., and Toksoz, M. N., 1995, Borehole wave propagation in three-dimensions: *J. Acoust. Soc. Am.*, **97**, 3483–3493.
- Corrigan, D., Withers, R., Darnall, J., and Skopinski, T., 1996, Fracture mapping from azimuthal velocity analysis using 3-D surface seismic data: 66th Ann. Internat. Mtg., Soc. Expl. Geophys., Expanded Abstracts, 1834–1837.
- Goff, J. A., and Jordan, T. H., 1988, Stochastic modeling of seafloor morphology: Inversion of sea beam data for second-order statistics: *J. Geophys. Res.*, **93**, 13589–13608.
- Hudson, J. A., 1981, Wave speeds and attenuations of elastic waves in material containing cracks: *Geophys. J. Roy. Astr. Soc.*, **64**, 133–150.
- Hudson, J. A., Liu, E., and Crampin, S., 1996, Transmission properties of a plan fault: *Geophys. J. Internat.*, **125**, 559–566.
- Johnson, D. H., and DeGraaf, S. R., 1982, Improving the resolution of bearing in passive sonar arrays by eigenvalue analysis: *IEEE Trans. Acous. Speech and Signal Proc.*, **AASSP-30**, 638–647.
- Liu, E., Macbeth, C. D., Pointer, T., and Hudson, J., 1996, The effective elastic compliance of fractured rock: 66th Ann. Internat. Mtg., Soc. Expl. Geophys., Expanded Abstracts, 1842–1845.
- Lynn, H. B., and Beckham, W., 1998, *P*-wave azimuthal variations in attenuation, amplitude, and velocity in 3-D field data: Implications for mapping horizontal permeability anisotropy: 68th Ann. Internat. Mtg., Soc. Expl. Geophys., Expanded Abstracts, 193–196.
- Lynn, H. B., Bates, C. R., Simon, K. M., and van Dok, R., 1995, The effects of azimuthal anisotropy in *P*-wave 3-D seismic: 65th Ann. Internat. Mtg., Soc. Expl. Geophys., Expanded Abstracts, 723–730.
- Mallick, S., Craft, K. L., Meister, L. J., and Chambers, R. E., 1998, Determination of the principal directions of azimuthal anisotropy from *P*-wave seismic data: *Geophysics*, **63**, 692–706.
- Mazzotti, A., 1991, Amplitude, phase and frequency versus offset applications: *Geophys. Prosp.*, **39**, 863–886.
- Neidell, N. S., and Cook, E. E., 1986, Seismic method for identifying low velocity subsurface zones: U.S. Patent 4 571 710.
- Parra, J. O., Hackert, C. L., and Xu, P. C., 2000, A model to relate *P*-wave attenuation to fluid flow in fractured tight gas sands: 70th Ann. Internat. Mtg., Soc. Expl. Geophys., Expanded Abstracts, 1919–1922.
- Paul, R. J., 1993, Seismic detection of overpressure and fracturing: An example from the Qaidam basin, People's Republic of China: *Geophysics*, **58**, 1532–1543.
- Perez, M., 1997, Detection of fracture orientation using azimuthal variation of *P*-wave AVO response: M.S. thesis, Massachusetts Inst. of Technology.
- Perez, M., and Gibson, R., 1996, Detection of fracture orientation using azimuthal variation of *P*-wave AVO responses: Barinas field (Venezuela): 66th Ann. Internat. Mtg., Soc. Expl. Geophys., Expanded Abstracts, 1353–1356.
- Perez, M., Grechka, V., and Michelena, R. J., 1999, Fracture detection in a carbonate reservoir using a variety of seismic methods: *Geophysics*, **64**, 1266–1276.
- Ramos, A. C. B., and Davis, T. L., 1997, 3-D AVO analysis and modeling applied to fracture detection in coalbed methane reservoirs: *Geophysics*, **62**, 1683–1695.
- Ruger, A., 1998, Variation of *P*-wave reflectivity with offset and azimuth in anisotropic media: *Geophysics*, **63**, 935–947.
- Schmidt, R., 1979, Multiple emitter location and signal parameter estimation: Spectral Estimation Workshop, RADC, Proceedings, 243–258.
- , 1986, Multiple emitter location and signal parameter estimation: *IEEE Trans. Antennas and Propagation*, **AP-34**, 276–280.
- Schoenberg, M., and Sayers, C. M., 1995, Seismic anisotropy of fractured rock: *Geophysics*, **60**, 204–211.
- Shen, F., 1999, Seismic characterization of fractured reservoirs: Ph.D. thesis, Massachusetts Inst. of Technology.
- Shen, F., and Toksöz, M. N., 2000, Scattering characteristics in heterogeneous fractured reservoirs from waveform estimation: *Geophys. J. Internat.*, **140**, 251–266.
- Tsvankin, I., 1996, *P*-wave signatures and notation for transversely isotropic media: An overview: *Geophysics*, **61**, 467–483.